



Finite Element Analysis of Lattice Structure Model with Control Volume Manufactured Using Additive Manufacturing

Ahmad Kholil¹, Gandjar Kiswanto^{1*}, Adnan Al Farisi¹, Jos Istiyanto¹

¹*Department of Mechanical Engineering, Faculty of Engineering, Universitas Indonesia, Kampus UI Depok, 16424, Indonesia*

Abstract. This study aimed to optimize lattice structure design by changing the size of unit cell at a constant volume. It was observed that the changes in unit cell affected the strength of lattice structure, posing a challenge for additive manufacturing. To evaluate these effects, Finite Element Analysis (FEA) was conducted by applying static loading at one end of the surface from x, y, z-axis, and combination of model, using Inconel 625 additive manufacturing. Furthermore, the model was analyzed by plotting graphs of changes in cell size to deformation and stress. The addition of outer skin to deformation and stress behavior was also investigated. Printed parts were manufactured through additive manufacturing using PLA to assess how changes in lattice size affected overhang surface quality. The results showed that deformation and stress behavior were influenced by the smallest cross-sectional area and shape of the unit cell, as shown by the relationships within lattice structure models. The addition of compression loads also increased deformation and stress behavior, while high outer skin thickness reduced these parameters in lattice model. The results from the printed part of model showed poor surface quality, particularly on the overhanging part.

Keywords: Additive manufacturing; Control volume; Design optimization; Lattice structure; Unit cell

1. Introduction

The topic of lattice structure design is one of the most active areas in additive manufacturing (AM) study. AM has the ability to produce complex lattice structure while maintaining geometry, optimizing the manufacturing of parts by the reduction in material without compromising the strength and deformation aspects. According to ASTM52900-21, AM is the process of joining materials to create parts from 3D model data, typically one layer after another, compared to subtractive manufacturing and formative manufacturing methodologies (Kiswanto, Kholil, and Istiyanto, 2023; ASTM-52900, 2021). Furthermore, it is a 3D printing technology with significant potential for revolutionizing various industries. This innovative manufacturing enables the production of complex and intricate structures that were previously unattainable through conventional processes such as casting, forging, and machining (Zhong *et al.*, 2019). The method allows 3D models drawn with computer-aided designs to be presented as functional products estimated during the early design phase quickly and efficiently (Saptaji *et al.*, 2022; Budiono, Kiswanto, and Soemardi, 2014).

*Corresponding author's email: gandjar_kiswanto@eng.ui.ac.id, Tel.: +62-21-7270032
doi: [10.14716/ijtech.v14i7.6660](https://doi.org/10.14716/ijtech.v14i7.6660)

Filament based-Material Extrusion Additive Manufacturing (FMEAM) is increasingly used as one of the prominent AM methods. In this method, polymeric materials are commonly preferred due to the low cost. However, metal filaments have been used, such as Atomic Diffusion Additive Manufacturing (ADAM) technology by Markforged. FMEAM with metal filaments is the mixing of metal powder particles with polymer binders to create a product applicable as a continuous feed in a 3D printer. This process is usually followed by a chemical and temperature treatment (Kiswanto, Kholil, and Istiyanto, 2023; Nurhuda *et al.*, 2021). In 3D printing, support structures are often needed to prevent the collapse of taller or smaller parts of the object during printing. Meanwhile, the removal of these structures after completion often requires a significant amount of material and time, leading to increased waste and higher production costs (Panesar *et al.*, 2018). One of the attractive applications of FMEAM is the fabrication of lattice structure, offering exceptional lightweight, high-strength, and energy-absorbing properties. Therefore, the importance of lattice structure design that can minimize the need for support structures becomes crucial in reducing material waste and conserving energy during the manufacturing process (He *et al.*, 2022; Nurhuda *et al.*, 2021; Haghshenas and Khonsari, 2018; Tang *et al.*, 2018).

Lattice structure is characterized by periodic arrangements of interconnected struts, creating a network of voids in the solid material. The structure has significant mechanical properties, such as high stiffness-to-weight ratio and enhanced energy absorption capabilities, allowing the suitability for various engineering applications (Benedetti *et al.*, 2021; Cheng, Bai, and To, 2019; Tang *et al.*, 2018). However, the intricate geometry and internal complexity pose significant challenges when analyzing mechanical behavior. Lattice structure also offers several advantages, including the provision of specific strength and stiffness to an object while significantly reducing material usage (Du *et al.*, 2020; Wang *et al.*, 2020; Zhong *et al.*, 2019; Yap *et al.*, 2015). These properties are essential in the design of objects in industries such as aerospace, automotive, medical, and other manufacturing fields (Dong *et al.*, 2020). A previous study on the triangular lattice structure of Inconel 625 observed a 57.6% reduction in impact toughness compared to the solid infill pattern (Kiswanto, Kholil, and Istiyanto, 2023). During the analysis, compressive test was conducted on SC, HC, BCC, and PG80 lattice structures (Seek *et al.*, 2022), while functionally graded lattice, including BCC and hexagonal HC structures, used photo-curable polyurethane resin (Park and Park, 2020). Despite the difference in volume, there is an insignificant comparison between models, as this approach is not apples-to-apples and profitable based on the volume of materials used. Consequently, this study presents a novel approach to controlling lattice volume.

In AM process, Computer-Aided Design (CAD) is crucial for designing the objects to be printed. However, creating effective lattice structure design using CAD software can be a challenge, particularly when there is a need for adaptation to specific AM technology such as MEAM. One of the main challenges includes the availability of free software that aids in designing product to create structure with the desired shape, size, and volume, in a short period (Barclift *et al.*, 2017). To address these issues, this study presents CAD module capable of automatically generating lattice structure based on Application Programming Interface (API). CAD API is an application programming interface that allows users to access and manipulate data in CAD software. CAD API tool has been developed using the Visual Basic programming language in SolidWorks software (Zhang *et al.*, 2019; Nguyen *et al.*, 2018) to facilitate the modification of unit cell and lattice structure parameters.

Finite Element Analysis (FEA) is a powerful tool for investigating the mechanical response of complex structures, providing valuable insights into the behavior under different loading conditions (Hamza *et al.*, 2023). This tool enables the prediction and

optimization of lattice structure performance before their physical realization (Cheng, Bai, and To, 2019; Tang *et al.*, 2018). Consequently, this study focuses on FEA application to analyze lattice structure models using Inconel 625 material additive manufacturing.

This study aimed to develop lattice structure model and perform FEA using the same unit cell, different sizes, and a constant volume. FEA was conducted on lattice structure models by providing static loading at one end of the model surface from x, y, z, and combination directions. Specifically, the material selected for FEA was Inconel 625 additive manufacturing. The effect of different sizes of unit cell on deformation and stress, including the addition of outer skin was investigated. Printed parts produced through FMEAM with PLA were verified to assess the quality of the overhang surface. This method was expected to reduce material, improve efficiency in the manufacturing process, and maintain high strength as well as low deformation. The consideration was used to optimize the manufacturing of parts in reducing material without minimizing the strength and deformation aspects. By comparing models with a constant volume, this study determined how changes in unit cell dimensions correspond to variations in strength and deformation.

2. Material and Methods

The initial step is designing a unit cell with a cubic base of different sizes while maintaining constant volume in lattice structure model. This model is considered due to its simplicity and versatility across several applications. By maintaining a constant volume comparison in FEA, it will provide an overview of changes in unit cell dimensions related to stress and deformation. As presented in Figure 1, the design of unit cell and the volume denoted as (1) is used as follows:

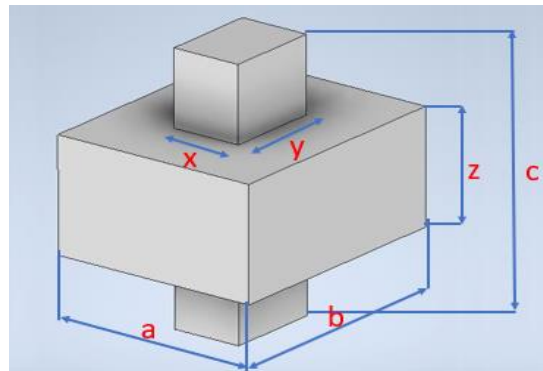


Figure 1 Unit cell design of lattice structure

$$V = abz + 0,5bx(c - z) \tag{1}$$

Where V is the volume (mm^3), and to achieve a constant volume, the parameters a , b , c , z , and y (mm) are fixed, while z and x are varied. The value of y is obtained from Equation 2 and x is derived from Equation 4.

$$y = \gamma b \tag{2}$$

Where: $\gamma = 0.1 - 0.9$

$$y = 0.5b \tag{3}$$

Where the parametric value of γ ranges from 0.1 to 0.9, but in this study, a value of $\gamma = 0.5$ is used. This value is selected as half the width of the unit cell and a fixed parameter in generating lattice models.

$$x = \frac{2(V-abz)}{b(c-z)} \tag{4}$$

The results of unit cells with varying sizes z and x , are shown in Figure 2. All unit cells have a constant volume of 1200 mm^3 , while the dimensions vary in z value from 8.8 mm to 6 mm with a change of 0.2 mm to obtain 15-unit cells. The value of x is taken from equation 4, while the values a , b , c , and y are constant.
















a = 10 mm; b = 12 mm; c = 14 mm; y = 6 mm; Vol = 1200 mm ³															
z (mm)	8.8	8.6	8.4	8.2	8.0	7.8	7.6	7.4	7.2	7.0	6.8	6.6	6.4	6.2	6.0
x (mm)	4.6	5.2	5.7	6.2	6.7	7.1	7.5	7.9	8.2	8.6	8.9	9.2	9.5	9.7	10.0
Area (mm ²)	40.48	44.72	47.88	50.84	53.60	55.38	57.00	58.46	59.04	60.2	60.52	60.72	60.8	60.14	60.00
Model															
	①	②	③	④	⑤	⑥	⑦	⑧	⑨	⑩	⑪	⑫	⑬	⑭	⑮

Figure 2 Size parameters of the unit cell

The design of lattice structure model with the same unit cell, different sizes, and a constant volume requires tools created in CAD software. API service was developed based on the Visual Basic programming through Solidworks. Figure 3a shows the interface of API service, which is used to input the parameter values of a , b , c , z , y , and V , where the value of x will be generated according to Equation 4. Subsequently, the input of the upper and lower base parameter values is followed by determining the number of unit cells in directions a , b , and c . Figure 3b shows lattice model generated from API service.

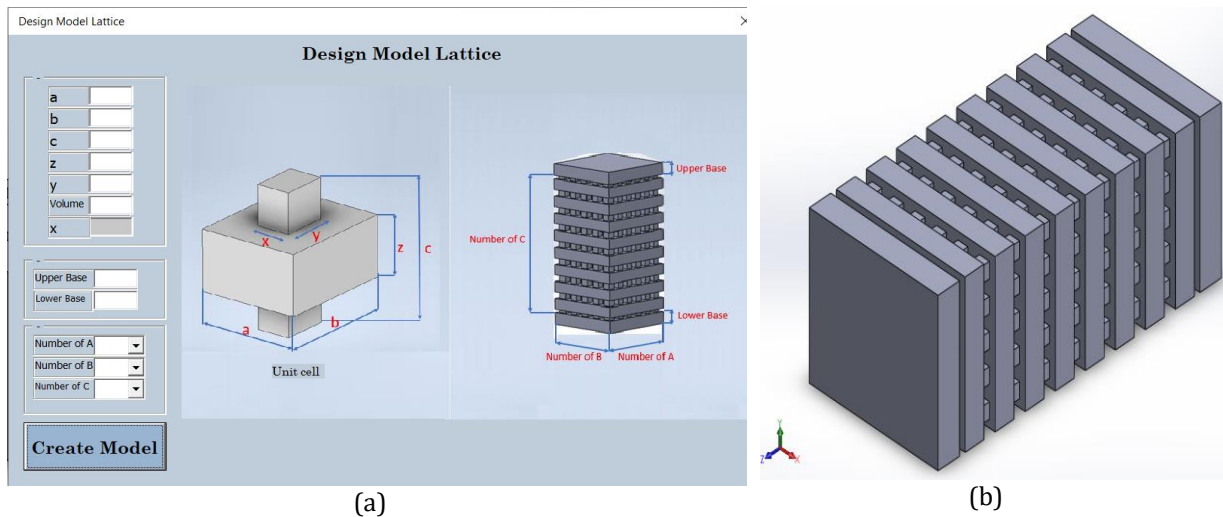


Figure 3 (a) The interface of parameters lattice structure, (b) model of lattice structure generated by API service

Figure 4 shows CAD model of lattice structure model generated through API service, using the data obtained from Figure 2. The number of unit cells in directions a , b , and c are 6, 5, and 8, respectively, resulting in a total of 240 unit cells forming lattice structure. The top and bottom bases are created with a size of 10 mm each. Each lattice model has a constant volume of $360,000 \text{ mm}^3$ with a total dimension of 60 mm x 60 mm x 132 mm. All lattice models have a constant mass of 3,038.4 g for each model. The unit cell of each lattice structure varies in z value from 8.8 mm to 6 mm with a change of 0.2 mm. In this study, 15 lattice structure models are obtained, as presented in Figure 4 for analysis.

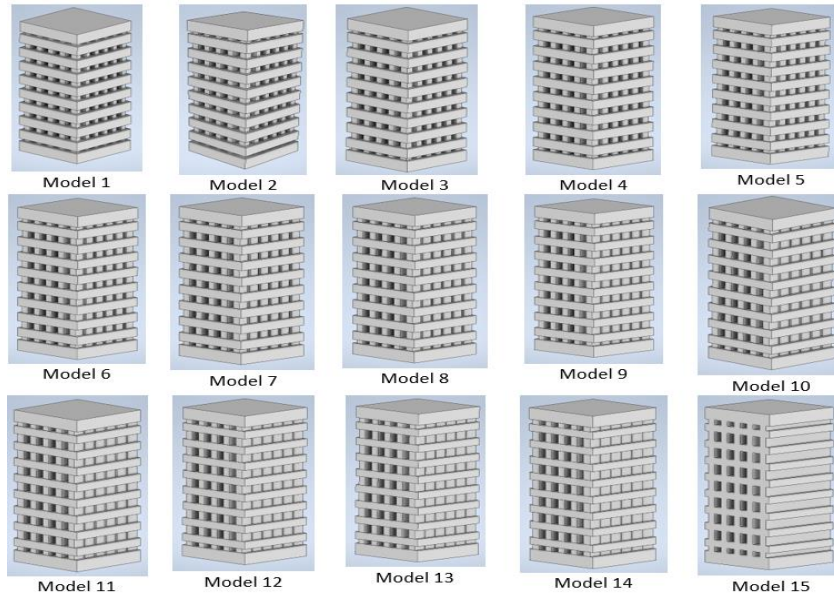


Figure 4 Lattice structure model generated by API service

FEA was conducted using ANSYS 2023 student version. Figures 5a-e show the boundary conditions of the simulation. One of the final surfaces of the models was given a fixed constraint, while the other in the front was given a force. The first simulation in Figure 5a applied forces in x-axis with a magnitude of 100 kN. The simulation was performed on 15 lattice structure models and 1 solid model. The material used was Inconel 625 Additive Manufacturing. The same boundary conditions were applied for all models in the second simulation, as shown in Figure 5b, with forces in y-axis at a magnitude of 100 kN. Similarly, the third simulation presented in Figure 5c applied forces in the z-axis with a magnitude of -100 kN. The fourth simulation in Figure 5d applied forces in xyz-axis with a magnitude of 100 kN. All simulations were performed on 15 lattice structure models and 1 solid model. Additionally, FEA was conducted with varying compression loads ranging from 100 kN to 1500 kN on lattice structure model, solid model, and lattice structure model with outer skin thicknesses of 1 mm, 3 mm, and 5 mm, as shown in Figure 5e.

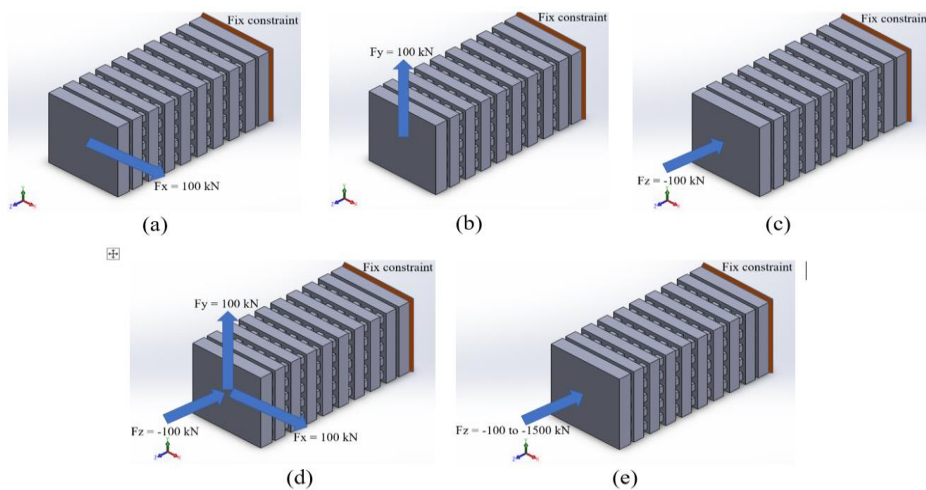


Figure 5 Boundary condition of FEA for lattice structure models with (a-d) loads in x, y, z-axis, and combination, (e) 100 – 1500 kN compression loads in the z-axis

The final step is printing pf all models through Flashforged with PLA material. Parameter settings are defined by layer thickness of 0.1 mm, extruder temperature 210°C, platform temperature 50°C, travel speed 80 mm/s, and without support.

3. Results and Discussion

FEA results of deformation for 15 lattice structure models and 1 solid model are shown in Figure 6. In x-axis and y-axis, the deformation curves showed the same pattern, obtaining the lowest values obtained by model 15 at 0.889 mm and 0.999 mm. For the z-axis, the lowest deformation was observed in lattice model 15, at 0.039 mm. In the combined xyz deformation, there was a significant decrease in deformation values from model 1 to 7, followed by a continuous reduction trend. Comparing the deformation results between the solid and lattice structure in the combined xyz, the solid model showed a value of 0.779 mm, while the smallest value was observed in lattice structure model 15, at 1.61 mm.

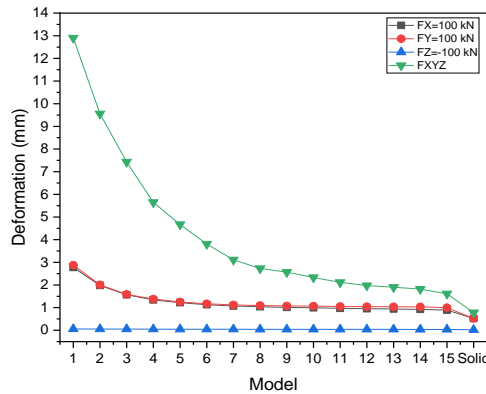


Figure 6 Deformation behavior was affected change dimension of unit cell under x, y, z, and combination loading

Figure 7 shows the results of stress behavior for the model. The maximum stress values in x, y, z-axis, and combination were obtained by model 1, at 771 MPa, 770 MPa, 102 MPa, and 1,315 MPa, respectively. These values decrease as the shape of the unit cell changes. In x-axis, the smallest stress was obtained by model 12, at 677 MPa, while y-axis had the smallest stress of 674 MPa obtained by model 13. For the z-axis compression, model 15 had the lowest stress, with a stress of 69.9 MPa. Regarding the combined xyz, the lowest stress value was found in model 12, at 702 MPa, while the solid model had 487 MPa on x-axis and y-axis, of 47 MPa on the z-axis, and 677 MPa in combination loads.

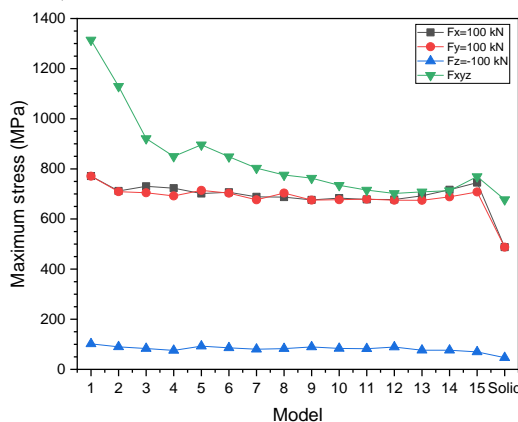


Figure 7 Stress behavior was affected change dimension of unit cell under x, y, z, and combination loading

The deformation and stress values were influenced by the smallest cross-sectional area of the unit cell, as shown in Figure 2. Model 1 has the smallest unit cell cross-sectional area, increasing to the maximum in Model 13, followed by a decrease in Model 15. The shape factor could also be influenced, particularly the load in x-axis or y-axis, and the combination, causing bending in lattice structure.

Figures 8 and 9 are FEA images of deformation and stress behaviors of model 1 under x, y, z, and combination loading.

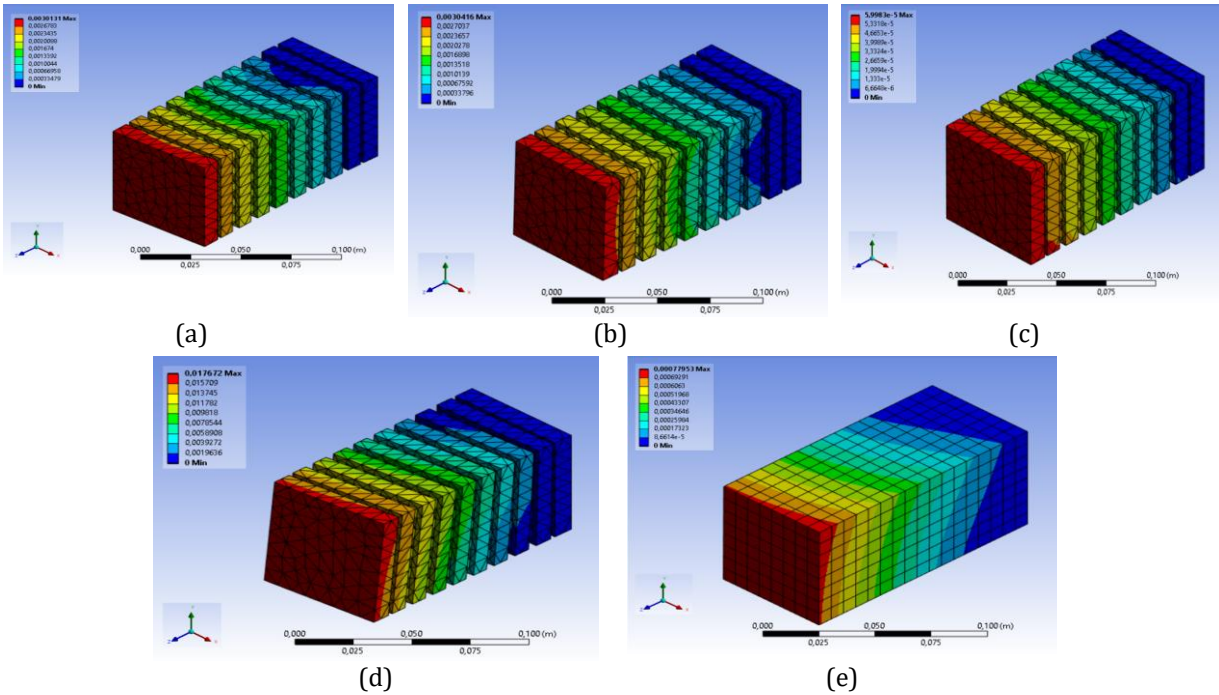


Figure 8 FEA result of deformation behaviors for loads: (a) $F_x = 100$ kN, (b) $F_y = 100$ kN, (c) $F_z = -100$ kN, (d) $F_{xyz} = 100$ kN, and (e) $F_{xyz} = 100$ kN of the solid model

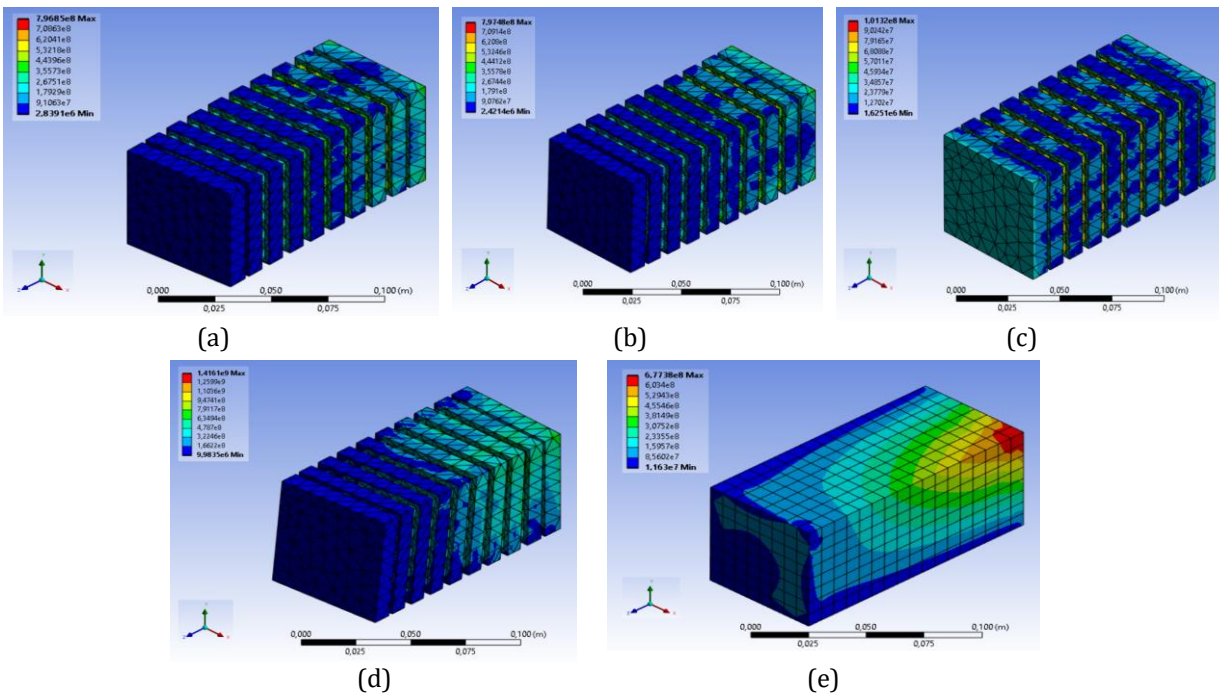


Figure 9 FEA result of stress behaviors for loads: (a) $F_x = 100$ kN, (b) $F_y = 100$ kN, (c) $F_z = -100$ kN, (d) $F_{xyz} = 100$ kN, and (e) $F_{xyz} = 100$ kN of the solid model

Figure 10a shows the results of maximum deformation for the solid model, lattice Model 5, and lattice Model 5 with an outer skin of 1 mm, 3 mm, and 5 mm, respectively. Under compression loads ranging from 100 kN to 800 kN, the five models did not show significant differences in deformation. However, as the compression load increased from

900 kN to 1500 kN, substantial differences were observed, showing an increasing trend with the addition of load for each model. At a compression load of 1500 kN, model 5 showed the highest deformation at 8.6 mm, followed by lattice models with outer skin thicknesses of 1.0 mm, 3.0 mm, and 5.0 mm, and the solid model, at 5.01 mm, 2.02 mm, 1.25 mm, and 0.34 mm, respectively. The results showed that increasing the applied compression load led to a rise in deformation, while higher thickness caused a significant reduction (Kumar *et al.*, 2020). Figure 10b shows the results of maximum stress for the solid model, model 5, and model 5 with outer skin of 1 mm, 3 mm, and 5 mm. As the applied load varied from 100 kN to 1500 kN, there was a trend of increasing stress for each model. Among the five models, at a load of 1500 kN, Model 5 has the highest stress, with a value of 1130 MPa. This was followed by lattice models with outer skin thicknesses of 1 mm, 3 mm, and 5 mm, and the solid model, showing maximum stress values of 941 MPa, 754 MPa, 738 MPa, and 699 MPa, respectively. The results showed that increasing the applied compression load improved maximum stress and energy absorption capability, while additional thickness in the outer skin caused a significant (Seek *et al.*, 2022; Kumar *et al.*, 2020).

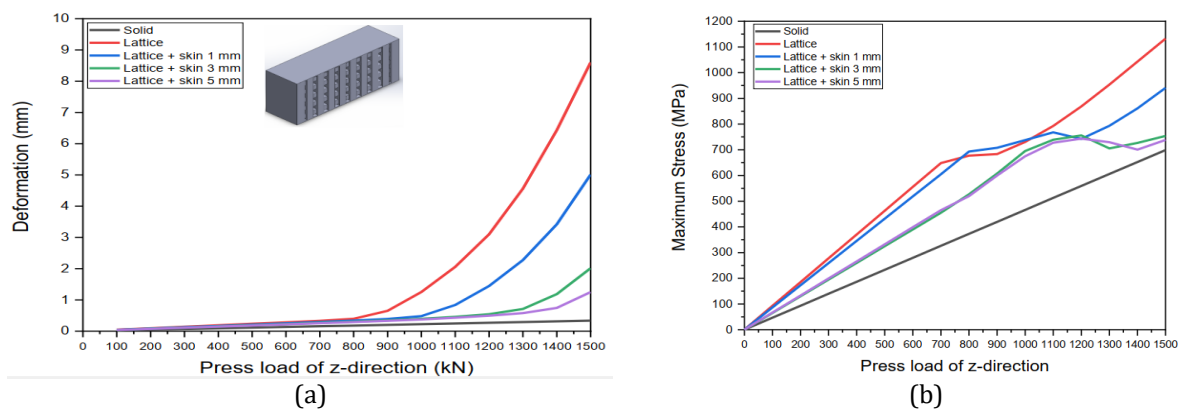


Figure 10 (a) Deformation, and (b) stress behavior of lattice model with outer skin under press loads of 100-1500 kN

Figure 11a-b shows the printed part of models 1-15 built through FMEAM. Verification of printing results with FMEAM using PLA was carried out to determine how changes in lattice size affected the quality of the overhang surface. As shown in Figure 11c, the overhang structure did not collapse, although support was not added. However, the surface quality is good compared to the structure that does not overhang.

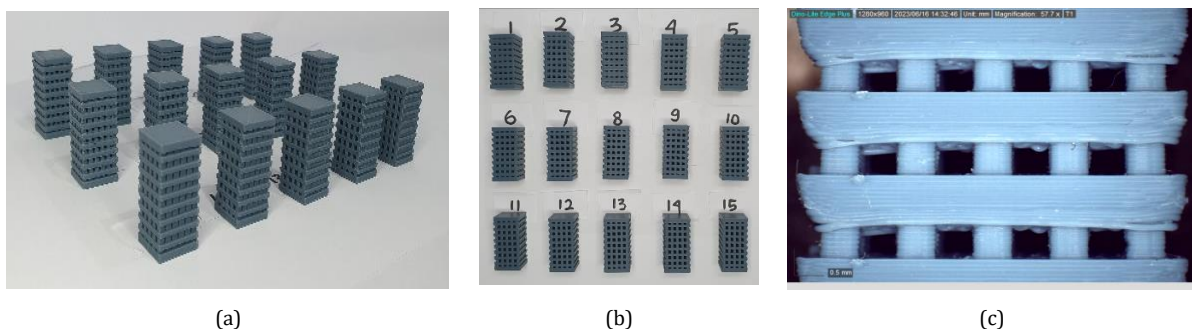


Figure 11 (a-b) model 1-15 built by FMEAM, (c) lattice models with overhang structure.

4. Conclusions

In conclusion, this study aimed to develop lattice model optimization method using the same basic unit cell shape with different sizes and a constant volume created by API service. This method was expected to reduce material usage and improve efficiency in the

manufacturing process while maintaining high strength and low deformation. The results suggested that changing the size of lattice cells at a constant volume affected the strength of the structure. Furthermore, changes in the dimensions of cell lattice models with x, y, z axis, and combined loading directly influenced deformation and stress. Lattice Model 15 had the smallest deformation and stress compared to the others. FEA results showed a considerable increase in deformation and stress, particularly in comparison to the solid. Increasing the thickness of the outer skin caused a reduction in the values of these variables. The printed models with FMEAM showed poor surface quality, specifically on the overhanging parts, but can be fixed through post-processing. Further studies should focus on establishing the optimal lattice models and thickness of the outer skin for a part such as a turbine blade.

Acknowledgments

The authors are grateful for the financial support from RIIM BRIN grant number: 97/IV/KS/11/2022. The authors are also grateful to the Engineering Faculty of Universitas Indonesia for providing Seed Funding Grant of 2022.

References

- ASTM-52900, 2021. *Additive Manufacturing—General Principles—Fundamentals and Vocabulary*. ASTM International
- Barclift, M., Armstrong, A., Simpson, T.W., Joshi, S.B., 2017. CAD-Integrated Cost Estimation and Build Orientation Optimization to Support Design for Metal Additive Manufacturing. *In: International Design Engineering Technical Conferences and Computers and Information in Engineering Conference*, Volume 58127, p. V02AT03A035
- Benedetti, M., Du-Plessis, A., Ritchie, R.O., Dallago, M., Razavi, N., Berto, F., 2021. Architected Cellular Materials: A Review on Their Mechanical Properties Towards Fatigue-Tolerant Design and Fabrication. *Materials Science and Engineering: R: Reports*, Volume 144, p. 100606
- Budiono, H.D., Kiswanto, G., Soemardi, T.P., 2014. Method and Model Development for Manufacturing Cost Estimation during the Early Design Phase Related to the Complexity of the Machining Processes. *International Journal of Technology*, Volume 5(2), pp. 183–192
- Cheng, L., Bai, J., To, A.C., 2019. Functionally Graded Lattice Structure Topology Optimization for The Design of Additive Manufactured Components with Stress Constraints. *Computer Methods in Applied Mechanics and Engineering*, Volume 344, pp. 334–359
- Dong, G., Tang, Y., Li, D., Zhao, Y.F., 2020. Design and Optimization of Solid Lattice Hybrid Structures Fabricated by Additive Manufacturing. *Additive Manufacturing*, Volume 33, p. 101116
- Du, Y., Gu, D., Xi, L., Dai, D., Gao, T., Zhu, J., Ma, C., 2020. Laser Additive Manufacturing of Bio-Inspired Lattice Structure: Forming Quality, Microstructure and Energy Absorption Behavior. *Materials Science and Engineering: A*, Volume 773, p. 138857
- Haghshenas, A., Khonsari, M.M., 2018. Evaluation of Fatigue Performance of Additively Manufactured SS316 Via Internal Damping. *Manufacturing Letters*, Volume 18, pp. 12–15

- Hamza, S., Heidari, M., Ahmadizadeh, M., Dashtizadeh, M., Chitt, M., 2023. Modification of Horizontal Wind Turbine Blade: A Finite Element Analysis. *International Journal of Technology*, Volume 14(1), pp. 5–14
- He, M., Li, Y., Yin, J., Sun, Q., Xiong, W., Li, S., Yang, L., Hao, L., 2022. Compressive Performance and Fracture Mechanism of Bio-Inspired Heterogeneous Glass Sponge Lattice Structures Manufactured by Selective Laser Melting. *Materials & Design*, Volume 214, p. 110396
- Kiswanto, G., Kholil, A., Istiyanto, J., 2023. Effect of Infill Pattern on Impact Toughness, Microstructure, and Surface Roughness of Inconel 625 Built via Filament-Based Material Extrusion Additive Manufacturing. *Journal of Manufacturing and Materials Processing*, Volume 7(3), p. 114
- Kumar, A., Collini, L., Daurel, A., Jeng, J.-Y., 2020. Design and Additive Manufacturing of Closed Cells from Supportless Lattice Structure. *Additive Manufacturing*, Volume 33, p. 101168
- Nguyen, D.S., Tran, T.H.T., Le, D.K., Le, V.T., 2018. Creation of Lattice Structures for Additive Manufacturing in CAD Environment. *In: 2018 IEEE International Conference on Industrial Engineering and Engineering Management (IEEM)*, pp. 396–400
- Nurhuda, A.I., Supriadi, S., Whulanza, Y., Saragih, A.S., 2021. Additive Manufacturing of Metallic Based on Extrusion Process: A Review. *Journal of Manufacturing Processes*, Volume 66, pp. 228–237
- Panesar, A., Abdi, M., Hickman, D., Ashcroft, I., 2018. Strategies for Functionally Graded Lattice Structures Derived Using Topology Optimisation for Additive Manufacturing. *Additive Manufacturing*, Volume 19, pp. 81–94
- Park, J.-H. Park, K., 2020. Compressive Behavior of Soft Lattice Structures and Their Application to Functional Compliance Control. *Additive Manufacturing*, Volume 33, p. 101148
- Saptaji, K., Khoiriyah, N., Utomo, M.S., Dwijaya, M.S., Nadhif, M.H., Triawan, F., 2022. Fabrication of Rigid Polyurethane Foam Lumbar Spine Model for Surgical Training using Indirect Additive Manufacturing. *International Journal of Technology*, Volume 13(8), pp. 1612–1621
- Seek, C.Y., Kok, C.K., Lim, C.H., Liew, K.W., 2022. A Novel Lattice Structure for Enhanced Crush Energy Absorption. *International Journal of Technology*, Volume 13(5), pp. 1139–1148
- Tang, Y., Dong, G., Zhou, Q., Zhao, Y. F., 2018. Lattice Structure Design and Optimization with Additive Manufacturing Constraints. *IEEE Transactions on Automation Science and Engineering*, Volume 15(4), pp. 1546–1562
- Wang, Q.S., Li, S.J., Hou, W.T., Wang, S.G., Hao, Y.L., Yang, R., Misra, R.D.K., 2020. Mechanistic Understanding of Compression-Compression Fatigue Behavior of Functionally Graded Ti–6Al–4V Mesh Structure Fabricated by Electron Beam Melting. *Journal of the Mechanical Behavior of Biomedical Materials*, Volume 103, p. 103590
- Yap, C.Y., Chua, C.K., Dong, Z.L., Liu, Z.H., Zhang, D.Q., Loh, L.E., Sing, S.L., 2015. Review Of Selective Laser Melting: Materials and Applications. *Applied Physics Reviews*, Volume 2, p. 041101
- Zhang, B., Goel, A., Ghalsasi, O., Anand, S., 2019. CAD-Based Design and Pre-Processing Tools for Additive Manufacturing. *Journal of Manufacturing Systems*, Volume 52, pp. 227–241
- Zhong, T., He, K., Li, H., Yang, L., 2019. Mechanical Properties of Lightweight 316L Stainless Steel Lattice Structures Fabricated by Selective Laser Melting. *Materials & Design*, Volume 181, p. 108076